LIMNOLOGY
and
OCEANOGRAPHY: METHODS

Limnol. Oceanogr.: Methods 3, 2005, 59–74

A three-axis fast-tow digital Video Plankton Recorder for rapid surveys of plankton taxa and hydrography

Cabell S. Davis[1], Fredrik T. Thwaites[2], Scott M. Gallager[1], and Qiao Hu[2]
[1]Department of Biology, Woods Hole Oceanographic Institution, Woods Hole, MA 02543-1541, USA
[2]Department of Applied Ocean Physics and Engineering, Woods Hole Oceanographic Institution, Woods Hole, MA 02543-1541, USA

Abstract

A new Video Plankton Recorder (VPRII) has been developed for rapid surveys of plankton and seston in the size range of 100µm–1cm. The VPRII system includes: 1) a high-resolution digital camera (1Mpixel, 10-bits, 30Hz frame-rate), 2) a fast towfish capable of tow speeds up to 12 knots and 3-axis motion for automatic undulation and ship-wake avoidance, small diameter tow cable and winch for deployment on coastal vessels, and 3) new interface software (*Visual Plankton*) for automatic identification of plankton to major taxa and visualization of these taxa together with hydrographic data in real time. Camera and strobe optics are laboratory-adjusted to select the field-of-view (5–20mm), and depth-of-field is objectively calibrated using a tethered organism (e.g., copepod) and automatic focus-detection software. The VPRII towfish comprises a fuselage, a fixed main wing, and three servo-controlled tail fins: port and starboard for dive, climb, and roll control and rudder for lateral movement. Placement of the strobe (starboard wing-tip), camera (fuselage nose), and cantilevered tow-bridle minimize disturbance of the imaged volume. Compared with typical net surveys in shelf areas, the VPRII counts more plankton per station, quantifies ubiquitous fragile forms, automatically identifies plankton to major taxa and measures their size, quantifies scales of patchiness down to a few cm, and displays high-resolution distributions of plankton taxa and hydrography while underway. The VPRII is available to researchers via the Woods Hole Oceanographic Institution ship instrumentation pool.

Pelagic marine ecosystems are characterized by variability in biotic and abiotic components across a continuum of time and space scales from microns to thousands of kilometers (Haury et al. 1978). Present monitoring of these ecosystems is done primarily by large-scale ocean surveys that use net and bottle sampling to collect specimens for quantifying distributional patterns (e.g., CALCOFI, Ohman and Smith 1995; MARMAP, Sherman 1980). While such surveys provide valuable information on species and life stages, their spatial resolution is necessarily limited, owing to long sample collection and processing times. Limited resolution of biological oceanographic data affects our ability to understand processes controlling pelagic ecosystem dynamics.

Acknowledgments

We thank the officers and crew of the R/V *Oceanus* for their support during field tests of the new VPR system. Engineers Pierre Tillier, Ken Peal, Nick Witzel, Ed Hobart, and Steve Faluotico made valuable contributions to the design and construction of the new VPR. Others involved in this project include Bob McCabe, Dick Edwards, Carlos Medeiros, Matt Naiman, Tracey Sutton, Andy Girard, Geoff Ekblaw, Craig Marquette, Paul Fucile, Frank Bahr, Al Bradley, Ned Forrester, Gary Stanbrough, Charlie Clemshaw, Ken Doherty, David Schroeder, and many more. This work was supported by NSF Grant OCE-9820099.

Acoustic and nonimaging optical samplers have been developed to provide high-resolution data on biomass and size composition, but these samplers do not give information on taxonomic composition. Acoustic samplers provide acoustic scattering data at multiple wavelengths, thus yielding size-specific biomass estimates of plankton and nekton (Holliday et al. 1989; Wiebe et al. 2002). The Optical Plankton Counter is a widely used instrument that provides high-resolution measurements of abundance and size distribution of suspended particles (Herman 1992).

New towed optical-imaging samplers have been developed to obtain high-resolution taxa-specific distributions of plankton. These samplers include the Ichthyoplankton Recorder (Froese et al. 1990; Lenz et al. 1995), the Shadowed Image Particle Profiling and Evaluation Recorder (SIPPER, Samson et al. 2001), and the VPR (Davis et al. 1992*a*, 1992*b*). The BIOMAPERII (Wiebe et al. 2002) combines a two-camera VPR with multi-frequency acoustics thereby allowing synoptic sampling of large areas for particle/plankton biomass, together with taxonomic characterization.

Data analysis for optical-imaging samplers has been largely a manual or semiautomated process (e.g., Davis et al. 1996). Advances in image processing (Tang et al. 1998) and pattern recognition of plankton have made it possible to automatically

quantify coarse taxonomic composition (and species in some cases) of plankton at sea in real time (Davis et al. 2004).

Despite these advances, significant problems have remained with the VPR system and with towed plankton samplers in general. In order to sample vertically as well as horizontally, samplers are often towyoed by hauling in and paying out cable with a winch. Such towyoing typically requires a larger cable (e.g., 0.68-inch or 17 mm) to facilitate proper level-winding and avoid cable cross-over on the winch, and it also causes significant cable wear. Moreover, the towyoing method requires a constantly alert winch operator who must be diligent to avoid hitting the bottom with the instrument during payout or two-blocking the instrument into the towing sheave during haul-back. Use of a large cable also requires a large winch, which precludes use on smaller coastal vessels.

In addition to problems associated with towyoing, towed instruments typically are deployed off the stern of the vessel, which means sampling in the wake, where small-scale plankton distributions are destroyed. To avoid sampling in the wake, the VPR has been towed off the side of the fantail from the crane boom (Davis et al. 1996), but logistically this method is more difficult than stern deployments, especially in higher sea states.

The VPR has been deployed on a V-fin and towyoed at ship speeds up to 8 knots (4 m/s), but this speed is slower than typical transit speeds of research vessels. This speed reduction is a significant problem, since it requires more ship time to conduct a given survey. It also precludes opportunistic sampling on research vessels of opportunity (e.g., those in transit).

Several undulating instruments exist that do not require towyoing, including Seasoar, Scanfish, Aquashuttle (Chelsea Technologies Group) and the miniBat (Guildline Instruments Inc). These instruments have been used extensively to collect oceanographic data, and they work well. These vehicles undulate, and some can be towed very fast (12.5 m/s). Since these vehicles have a single-axis dynamic control surface, they do not have dynamic lateral control capability and, therefore, cannot be flown off to the side out of the ship's wake. They could conceivably be retrofitted with a fixed rudder to tow them off to the side, out of the ship's wake. However, this configuration would cause the vehicles to tilt horizontally at a substantial angle when near the surface so that vertically oriented plankton such as copepods would be imaged end-on rather than from the side, making identification more difficult. In general, these vehicles were not designed to be towed laterally, and lack of roll stability would be a problem in such cases.

Instrument packages are mounted in or on the fuselage of these undulating vehicles, which is problematic for the VPR imaging system, because the wake of the bridle and tow cable would disturb the imaged volume and cause avoidance by zooplankton. (The bridle is fixed in the vertical center-plane of the towbody on these vehicles).

A three-axis towed vehicle, Triaxus (MacArtney A/S), has been developed and used for oceanographic sampling. This vehicle has vertical as well as lateral motion control and can be used to sample off to the side of the ship out of the wake. This vehicle has a box-kite shape with the control fins at the edges of the box. Like other samplers, the tow bridle is attached at the center of the front of the towfish and therefore the cable/bridle wake would interfere with the VPR's image volume. There is no "undisturbed" region on this vehicle where the VPR could be mounted.

Aside from deployment and towing difficulties, the VPR image acquisition and processing system, as previously reported (Davis et al. 1996; Tang et al. 1998), was a prototype system and required significant user input. Also, the original VPR used analog video cameras that have a relatively low resolution and dynamic range. Video fields were digitized at 256 × 512 pixels and 8 bits per pixel (i.e., 256 gray levels). This lower pixel resolution limits the image volume and contrast range that can be sampled compared to more recent higher resolution cameras. These analog cameras also required an analog-to-digital frame grabber to capture the images, and electrical interference can be introduced to the analog signal prior to digitization, resulting in noisy images. Finally, although the image processing and analysis methods developed for the VPR allowed for automatic identification of plankton taxa and plotting of their distributional patterns in real time, this prototype system required significant user knowledge and setup time and was cumbersome to use.

To solve these problems, we have designed, built, and tested a VPRII system that (1) has a high-resolution digital video camera, (2) has a computer-controlled maneuverable three-axis towfish that can be undulated and flown off to the side of the vessel away from the wake, (3) can be towed at high speeds (e.g., 5 to 6 m/s), (4) minimizes disturbance of the image volume by locating the tow bridle on the opposite side of the towfish, (5) uses a small-diameter tow cable and small winch, so that it can be deployed from both small (15 m) coastal vessels as well as large research ships, (6) has improved user-friendly image processing and data analysis/display software for observing abundance patterns of plankton. The new system has been made freely available to the general oceanographic community when using Woods Hole Oceanographic Institution (WHOI) research vessels.

Materials and procedures

The VPRII system includes a towfish with flight control and data acquisition computers and shipboard computers for supervisory control and data logging, processing, and visualization (Fig. 1).

The towfish is similar to a fixed wing aircraft, with tail rudder and port and starboard tail fins that are used as ailerons and elevators (Figs. 1, 2). It is towed by a rigid bridle arm extending from the port side of the nosecone. Using this configuration, the towfish can be launched through the stern A-frame and flown off to starboard, out of the ship's wake. The

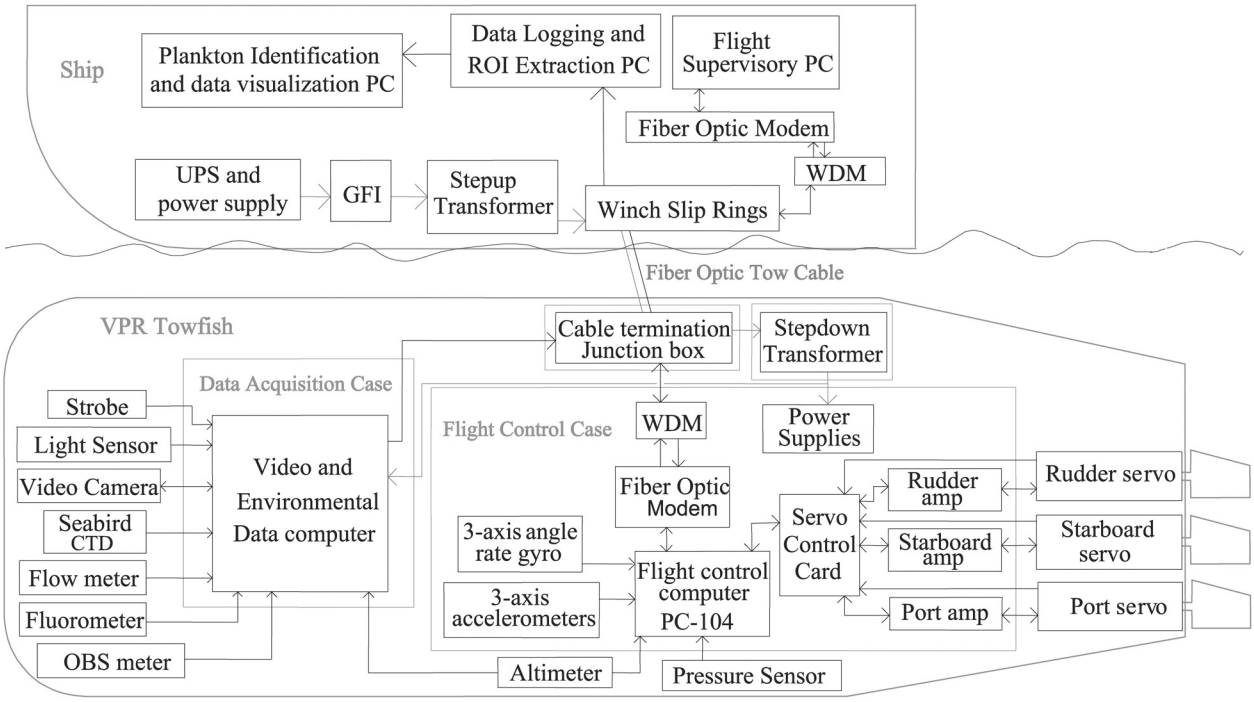

Fig. 1. Block diagram of the VPRII system showing shipboard and towfish components. UPS, uninterruptible power supply; GFI, ground fault interrupter; PC, personal computer; ROI, region of interest; WDM, wave division multiplexer; CTD, conductivity, temperature, depth sensor; OBS, optical backscatter. (redrawn from Thwaites and Davis [2002])

image volume is between the starboard wing tip and nose cone, away from the bridle arm and tow cable.

The towfish contains two primary subsystems: one for flight control and the other for plankton video and environmental data acquisition (Figs. 1, 2). Key design criteria include fast towing speed, computer-controlled three-axis motion with roll stability, and minimized hydrodynamic disturbance of the image volume. The towfish was designed to be towed at speeds up to 10 knots and has been tested extensively at 12 knots. The towfish measures $2.6 \times 2.0 \times 0.6$ m (L × W × H), has an air weight of 400 kg, and is ballasted with closed-cell foam to be near neutral buoyancy and level in seawater. The strobe housing is mounted inside the starboard wing tip cowling, and the camera is housed 90 cm away inside the fuselage nosecone (cf. Fig. 2A,B). The wing tip cowling is made of aluminum pipe and protects the strobe from damage. The towfish chassis is made from 3.81-cm hollow aluminum square stock welded together to form a sturdy and rigid frame. A single, large (10 cm diameter) aluminum pipe, running crosswise through the fuselage, forms the strength member for both wings (Figs. 2B, 3A). The wings themselves are fixed in position and are made from a baffled aluminum frame filled with rigid polyvinylchloride foam and covered with a rough fiberglass skin to keep the boundary layer attached at high angles of attack. The entire towfish is covered with a molded fiberglass cowling and is coated with flat black paint to minimize detection by plankton. The approximate position and size of the imaged volume is shown by the yellow dash in Fig. 2C,D (image volume calibration is discussed below). The fins consist of an aluminum skeleton covered with polyvinylchloride foam and fiberglass. Aluminum tail, wing skids, and rings on the wing tips protect the towfish from damage and are used as tag-line attachment points during deployment and retrieval.

The towfish is towed by a cantilevered bridle arm attached to the tow cable (Figs. 2, 3). The bridle arm is attached to the towfish via a universal joint at the midpoint of the wing spar. The bridle, made from 8.9 cm steel pipe, extends laterally outward through a semicircular opening on the port side of the fuselage nosecone and runs forward, with two additional bends, to the front of the towfish. As the towfish is flown to starboard, the bridle and cable move toward port, away from the nosecone and image volume (Fig. 3A). The angular range of vertical motion of the tow bridle is 145° (Fig. 3C). The frontal area of the nosecone tip and wing tip are relatively small (Fig. 3B), and the long nosecone and 1 m distance between it and the starboard wing tip, leave a large, open region around the image volume.

The tow cable (Rochester Cable Inc.) has a double-armored steel jacket, an outside diameter of 8.18 mm (0.322 inches), and is very robust. The cable has three optical fibers each wrapped with a copper conductor. Hard plastic flex-nose fair-

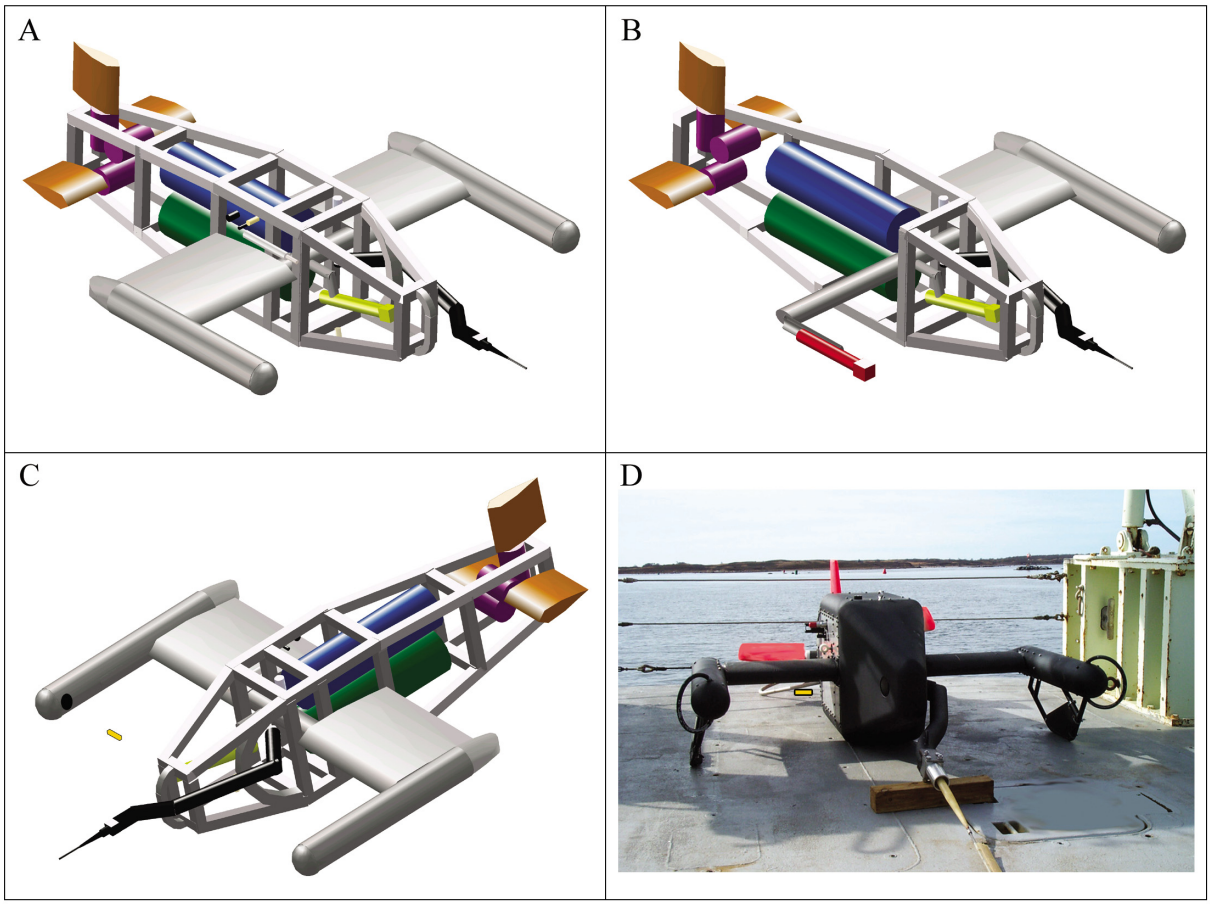

Fig. 2. The VPRII towfish. (A) Color-coded computer drawings showing the major components inside the towfish chassis. (B) As in A but with sections of chassis removed to allow viewing of components, including strobe (red), camera (gold), video/environmental data acquisition subsystem (blue), flight-control subsystem (green), servos (violet), fins (orange), and tow bridle arm (black). (C) Rotated view showing the bridle arm extending from the universal joint at wing center and extending outward through the semicircular opening in the fuselage nose. (D) The completed towfish with fiberglass cowling covering the chassis and painted black for stealth. The strobe is mounted in the starboard wing pontoon, while the camera is mounted 1.0 m away in the fuselage nose cone. Environmental sensors are mounted on the side of the fuselage above the wing. Yellow dash in C and D indicates approximate position and size of the image volume.

ing is used on the tow cable (Fig. 3D), which reduces drag by a factor of 25. The tow cable is attached to the end of the bridle using epoxy poured inside a steel termination and bolted to the bridle. The termination itself has a bell-mouth to distribute cable bending when the cable is under tension while towing, and a polyurethane strain relief is used to distribute bending and absorb vibration. The core of the tow cable (after removing the steel armor) is fed through the hollow bridle arm to a 3-cm hole in the arm near to where the bridle attaches to the towfish (i.e., near the universal joint). The cable core then is fed into an oil-filled junction box mounted in the towfish nosecone. Power and fiber optic connections between the towfish and the tow cable are made inside this junction box.

One of three optical fibers in the tow cable is used to send high-bandwidth video and environmental data from the towfish to the ship. Bidirectional data transmission between the shipboard supervisory computer and the towfish flight control computer is achieved using a wave-division multiplexer (WDM) to send data back and forth over a single optical fiber, saving the third fiber as a spare. Although this flight-control bandwidth is low (19,200 baud), fiber optic transmission was used because the copper conductors are used for power transmission.

In the winch drum, the end of the cable passes into a junction box connecting the fiber and copper conductors from the cable to leads from an electro-optical slip ring. Two fiber optic deck cables and a power cable then pass from the slip rings to the ship's lab. The flight control data on one optical fiber passes through a WDM, into a fiber optic modem, and into the supervisory computer (Fig. 1). The other optical fiber, carrying video and environmental data, is plugged into the data-logging computer.

The copper leads in the tow cable are small and have a high impedance over long distance (~1 km), and in order for the towfish to receive its required 1 kW of power, a high surface

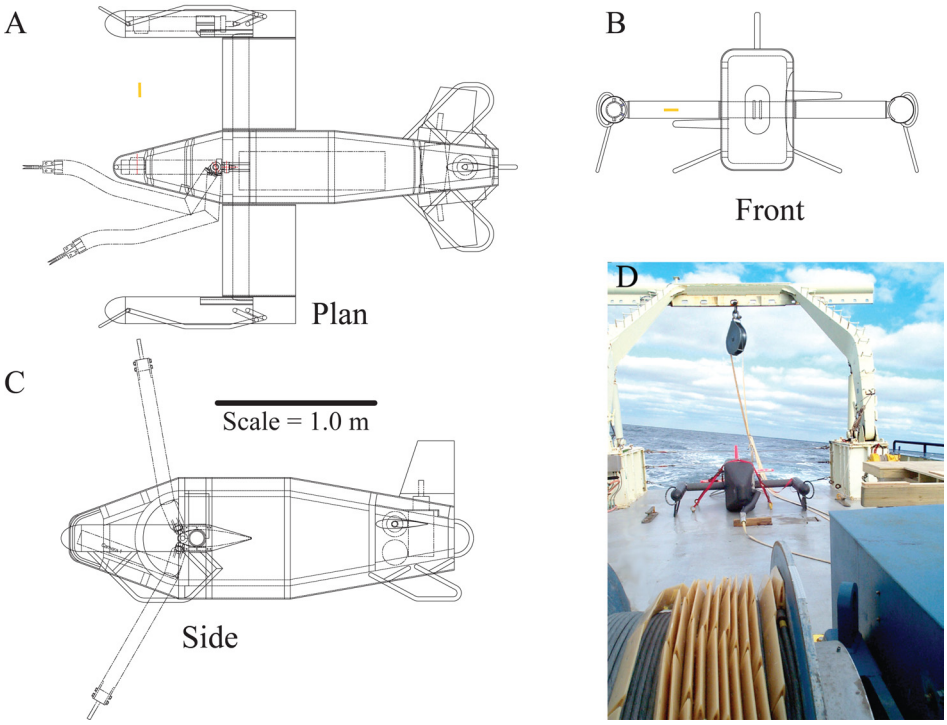

Fig. 3. (A-C) Computer-aided design line drawings of the towfish. Drawings are to scale. The two positions of tow arm bridle show its range of motion. Note also tail and wing skids (not shown in Fig. 2A-C). (Scale same for A-C). (D) Stern deployment configuration showing winch, cable with fairing on first 50 m, A-frame with sheave, and towfish (shown strapped to deck).

voltage (700 V AC) is needed. This voltage is supplied using a step-up transformer on clean power supplied by an uninterruptible power supply (Fig. 1). On the towfish end of the cable, the power passes through a step-down transformer that has three separate 110 V AC output windings that reduce coupling of noise from the servo amplifiers to the computer and analog measurement systems.

The tow cable passes through a specially made aluminum block with a 10-cm wide Nylatron sheave that allows the fairing to pass through without damage. The sides of the sheave itself are recessed inside the cheeks of the block, so that there is no chance for the tow cable to jump off the sheave and ride on the axle. The cable is wound on the drum of a 30-hp electro-hydraulic winch (Seamac Inc), which runs on 440 V 3-phase power. For our test cruises, we used an 800-m length of tow cable and paid out 700 m, leaving at least 1.5 wraps of cable on the winch drum while towing. Fairing was placed on 50 m of tow cable closest to the towfish, so that when the cable is wound on the winch drum, the last full wrap of cable is faired.

The VPRII is launched through the stern A-frame while the ship is steaming at 3 m/s. The tail dive planes are set in an upward position during launch so that the towfish skims on the surface after reaching the water. Prior to launch, tag lines are run through the aluminum rings on the wing tips, and slack in the tow cable is pulled out using the winch. Insulated lineman's gloves are worn for safety when handling the tow cable, which carries 700 V AC to the towfish (a floating ground and ground fault interrupters are used, as well). The towfish then is raised with the winch as the A-frame is moved astern. Once in the water, the towfish skims at the surface as the faired portion of the cable is deployed, after which the towfish is commanded to fly at 5 m depth while the rest of the 700 m of cable is paid out. Once the cable has been deployed, the winch is turned off and its brake applied. The towfish then can be commanded to operate in a desired sampling mode.

Recovery of the VPRII is also done through the stern A-frame. Lines are fed from two air tuggers, mounted near the A-frame base, through holes in cleats on the A-frame arms and attached to snatch hooks on long aluminum poles. The VPRII is brought close to the stern by hauling in cable with the winch, while steaming at 3 m/s, and tag lines are hooked onto the wing-tip rings. The cable is wound onto the winch, making sure the fairing is snugly stacked. With the A-frame in full aft position, the winch operator hauls the towfish out of the water as the A-frame is moved forward.

The flight-control computer in the towfish is preprogrammed with five flight modes, including surface skim, constant depth, undulate, abort, and manual flight. The shipboard supervisory computer contains a flight simulator-style interface (dubbed *Flyer*) that displays the pitch and roll of the

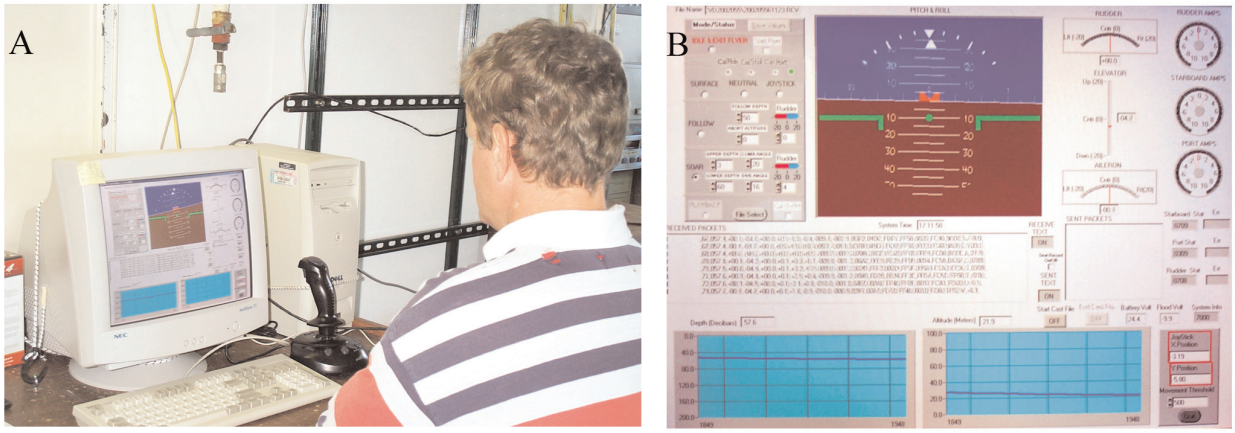

Fig. 4. Supervisory flight-control. (A) A shipboard supervisory computer displays flight data and allows the operator to select between flight modes (e.g., undulate). This computer relays the request to the flight-control computer inside the towfish, which switches to the commanded flight mode. The joystick can be used for manual control at speeds (<4 m/s). (B) User-interface window of the Flyer program showing the "horizon" sub-window (top center) as well as mode selection controls (upper left), numerical data stream from flight sensors (middle left), plots of towfish depth and altitude (bottom), and rudder/elevator/aileron positions and servo amps (upper right).

towfish, among other variables, and is used to select between the different sampling modes (Fig. 4). Once a mode is selected, the supervisory computer sends the command to the towfish flight computer telling it to switch to that mode. The towfish computer (PC-104) runs a 10-Hz dynamic control loop, which includes receiving data from the 3-axis angle-rate gyros, the 3-axis accelerometers, the pressure sensor (Paroscientic Inc., model 8CDP700), and altimeter (Benthos, model PSA-916); processing the data; and sending fin angle commands to the servo control card (ACS Tech 80 5940). This card communicates with the amplifiers supplying directional amperage to the three servos in a 2500-Hz control loop, maintaining fin angles at commanded values.

In surface skim mode, the fins are held in the full up position, causing the towfish to stay at the surface. In constant depth mode, the towfish automatically follows a depth specified by the operator via the shipboard supervisory computer. In undulate mode, the towfish automatically oscillates between two depths specified by the operator. In abort mode, when the towfish is in danger of hitting the bottom or fishing gear, a set climb rate is used together with zero rudder and roll angle, forcing a rapid ascent without overstressing the cable. Finally, in manual flight mode, the operator flies the towfish manually using a joystick. The manual mode is sometimes useful during launch or at slower speeds (4 m/s), but cannot be used at higher speeds because a human operator has a very difficult time controlling pitch with the speed over 4 m/s, owing to the latencies in the joystick mode.

The towfish subsystem for plankton video and environmental data acquisition consists of a digital CCD camera (Pulnix Inc, model 1040), strobe (Seascan Inc), conductivity-temperature-depth (CTD) (Seabird Inc., 16 Hz Fastcat), fluorometer (Seapoint Inc, model SCF), optical backscatter sensor (Seapoint Inc, model STM), photosynthetically active radiation (PAR) sensor (Biospherical Instruments., QCP-200L), and a data acquisition and telemetry computer (Figs. 1, 2). Initially, a Falmouth Scientifics Inc. CTD was used on the VPRII, but because it is not pumped and the towfish moves rapidly through the water, the lag in response times between temperature and conductivity sensors caused significant salinity spiking. We subsequently switched to a Seabird Inc. FastCat CTD that is pumped and outputs data at 16 Hz. This CTD is mounted externally on the starboard instrument panel. In addition to the above sensors, this subsystem also has pitch and roll sensors (Honeywell Inc.) and receives data from the altimeter (this subsystem can also be used on other sampling platforms). The camera is progressive scan monochrome 1008 × 1018 pixel CCD that outputs digital images at 30 frames per second via an RS422 interface. The data acquisition/telemetry computer, running an embedded Windows NT operating system, receives data from the sensors and telemeters it via a fiber optic transmitter to the ship. Digital video from the camera is received by a capture card (Matrox Inc., Meteor II Digital) interfaced to the computer. Incoming sensor data pass through A/D converters or are in RS232 format (CTD). Each video field captured by the computer is combined with the available sensor data and sent at the 30 Hz frame rate to the fiber optic transmitter card (Systran Inc, FibreXtreme), where it is sent through a short fiber optic cable to the oil-filled junction box in the nosecone of the towfish. Inside the junction box, this optical fiber is connected to one of the three optical fibers from the tow cable (ST connector).

The 20 W strobe (Hamamatsu xenon bulb L7684) flashes at 30 Hz in synchrony with the shuttered camera, such that the 2 μs light pulse occurs during the 1-ms camera shutter opening. This short shutter time effectively eliminates any contamination by ambient light. The strobe and camera housings

both contain 45° mirrors so that the housings point forward, whereas the camera and strobe optics are aligned toward each other (Figs. 2, 3). The optical axes of the strobe and camera are aimed slightly downward from horizontal, such that the main strobe beam passes adjacent to the window of the camera housing but not directly into it. Plankton are imaged from the forward scattered light generated by this off-axis illumination scheme (Davis et al. 1992*a*). Camera optics includes a manual zoom lens (Cosmicar/Pentax, model C31204, 12.5 to 75 mm, F1.8, 2/3 format) with an optical doubler and extension tubes: the exact configuration determining the magnification and working distance. A typical optical configuration includes the doubler plus 50 mm of extension tubes and lens settings of F11, closest focus, and full zoom. This configuration yields a 12-mm field of view, with the center of focus 50 cm from the camera housing faceplate. The lens f-stop affects the depth of field, and typically this depth is much greater than the field of view. An f-stop of 16 can yield a 10-cm depth of field, but often the circle of confusion resulting from this small aperture causes blurring of the image. Thus, an f-stop of 11 is often most suitable and yields a depth of field of 5 cm. Although the depth of field is relatively large, it remains shorter than the intersection of the strobe beam with the camera's optical path, leading to objects being illuminated but out of focus. It is important, therefore, to measure the depth of field. Once the illumination and optics are aligned, the imaged volume dimensions are calibrated.

The calibration procedure involves hanging the towfish by its tail with the nose and right wing tip immersed in a polyethylene seawater tank ($1.5 \times 1 \times 0.5$ m, L × W × H). A millimeter-ruled micro-positioning rail is mounted to the camera housing, parallel with the optical axis. A copepod or other plankton is tethered to a small (~200 µm) diameter black wire or hair using cyanoacrylate glue (e.g., Superglue or medical glue). The tether itself is made by placing a 3-cm length of the wire into the tip of a Pasteur pipette and securing it with glue. Copepods to be tethered are pipetted onto laboratory tissue paper, and the tether tip, with a very small amount of glue on it, is touched gently to the dorsal cephalothorax. The pipette with tethered copepod is inserted through a snug hole in the screw cap of a plastic test tube containing seawater. When the calibration hardware is set up, the pipette with tethered copepod is removed from the test tube, attached to the micro-positioning stage, and centered in the camera field of view. The micro-positioning stage then is moved along the optical axis while running the focus detection program (see "Image processing") to objectively determine the position of the near and far focal planes. The focal planes also are measured at each corner of the field of view. The width and height of the field of view are measured using a translucent plastic rule. Since the depth of field is ~5 cm, and the image volume is centered at a distance of ~60 cm from the camera lens, the size of the field of view changes by only ± 4% from the center of focus. Once the depth of field has been mapped, the strobe mirror can be rotated slightly to center the image volume in the strobe beam. The VPR typically is calibrated prior to each cruise, but the calibration will hold unless adjustments are made to the optical system.

Video and environmental data from the towfish are received via a fiber optic deck cable into the data-logging and region of interest (ROI) extraction computer (Fig. 1). Environmental sensor data accompanying each video frame are written as hourly files containing 30 Hz data lines in hexadecimal. This computer also receives navigational and bathymetry data from the ship at 1 Hz and combines it with a 1-s running average of the 30 Hz environmental data into a single log file for each tow.

Image processing—VPRII data processing involves focus detection, feature extraction, classification, and data display (Fig. 5).

Video frames are processed in real time and in-focus ROIs are detected and saved to disk in hourly folders as tiff files, with the file names containing the millisecond time of day that the video frame was captured (Fig. 5). For focus detection, the video first is corrected for uneven illumination using a running average of 500 frames. Each image then is segmented (binarized) at a user-selected brightness threshold. White regions (blobs, binary large objects) are detected and those above a minimum size are used as a mask on the original image to determine the gradient in grayscale in that ROI as a measure of its focus level. If the focus level is above the user-specified threshold, the ROI of the original image is saved to disk. Full detail of VPR ROI extraction method is given elsewhere (Davis et al. 1996, 2004).

ROI extraction and data logging (Figs. 1, 5) are accomplished using a stand-alone program (*VPRdeck*) written in C++. This program is used to read and display incoming data streams from the towfish (and ship global positioning system), extract, display, and save ROIs from the video, and write log files containing the sensor and navigation data. The *VPRdeck* interface window allows the user to select thresholds for brightness, focus, object size, and other parameters that determine the image volume during calibration.

Once ROIs are captured, a subset is copied for training. Training ROIs are manually sorted to yield approximately 200 per taxon. Features are extracted from the sorted training ROIs and the resulting feature vectors are used to build a classifier, either neural network or support vector machine. All ROIs then are feature-extracted and classified automatically and very rapidly (e.g., 5 ROIs/s on a 2-GHz Pentium 4), with the identification results being written into hourly files for each taxon. The features extracted and used for classification include shape-based (moment invariants, granulometry, roundness, Fourier descriptors) and texture-based (co-occurrence matrices) and are described in detail elsewhere (Tang et al. 1998; Davis et al. 2004: Hu and Davis, in press). Accuracy of machine classification for 7 to 10 taxa is 60% to 90% depending on taxa, which is sufficient to quantitatively measure abundance of dominant or distinctive taxa. This accuracy is the number of correctly identified images divided by the total and includes images unidentifiable by a human (typically 1/5 of total). A detailed

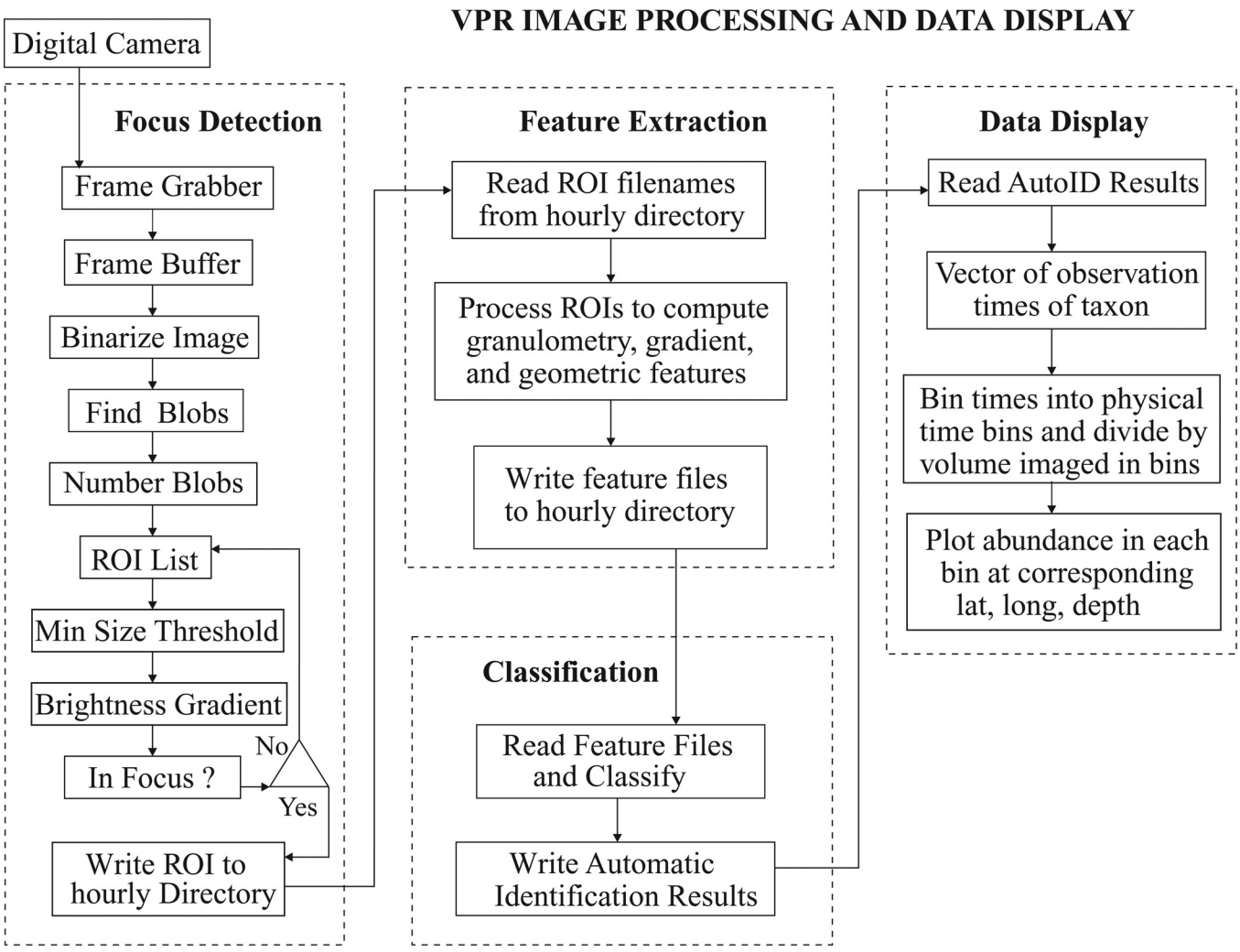

Fig. 5. Flow chart of VPR image processing and data display program.

analysis of classification accuracy using this method is given in Davis et al. (2004) and Hu and Davis (in press).

To plot the automatically classified data for a given taxon, the list of times that it was observed is obtained from the hourly filename lists for that taxon and converted to decimal year day in Greenwich Mean Time (GMT). Data from the navigation and sensor log file are read and parsed, and decimal year day in GMT is calculated for each row of data. The lists of times for the given taxon then are binned into the time bins corresponding to the rows of the sensor log file. The number of individuals observed in each time bin is divided by the total volume imaged during that period. For example, if the image volume is 7.2 mL and a time bin is 1 s, then, because the frame rate is 30 Hz, the VPR sampled 216 mL and the number of individuals counted during that 1-s time bin is divided by 0.216 L to compute abundance as individuals/L.

The primary interface program for video and environmental data acquisition, processing, and display is *Visual Plankton* (Fig. 6). This program was designed to streamline setup and use of the VPR by guiding the user through five main steps, including calibration, focus detection, classifier training, automatic classification, and data display (Fig. 6). The program was written in Matlab (Mathworks Inc). Clicking on a step in the main window and pressing *Apply* brings up a popup window for that step. The calibration window is used for entering the width and height of the field of view as well as near and far focus distances for the center and corners of the field of view. The focus detection window describes the procedure for running the *VPRdeck* program to extract ROIs and log data during sampling. The classifier training window simplifies the copying of training ROIs, selection of taxa to use in training, and building of the classifier. The automatic classification window allows the user to enter the day and hours containing ROIs that are to be classified. The data display window allows the user to select which sensor and plankton data to plot. It also allows for the option of manually correcting the automatic

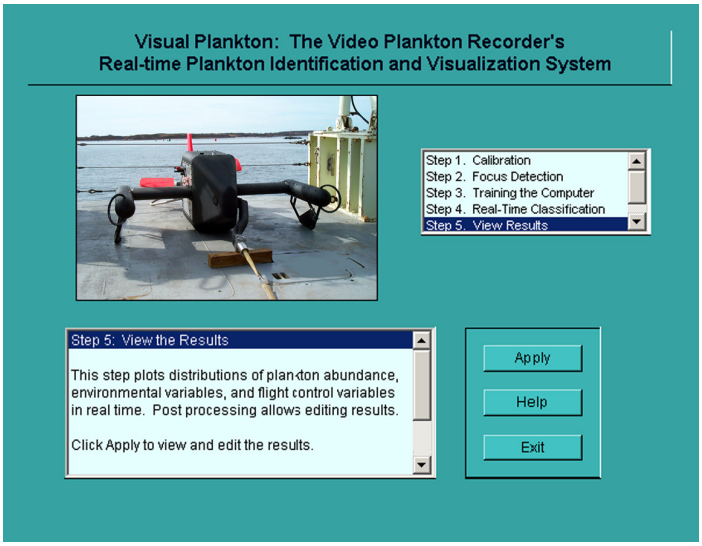

Fig. 6. Main window of the VPR data processing and display program *Visual Plankton*.

identification results, using a point-and-click graphical user interface.

Assessment

We conducted initial test trials of the new VPR aboard the R/V *Oceanus* (OC373) in waters off Woods Hole, Massachusetts, at two primary locations: the Gulf of Maine and the shelf/slope water south of Nantucket during February 2002 (Fig. 7.). The VPR was tested at a range of towing speeds from 1 to 6 m/s to assess the ability of the dynamic control system to perform the programmed sampling modes. At speeds slower than 3 m/s, the towfish is difficult to control because of its relatively small wing area, but at speeds from 3 to 6 m/s, the towfish flies well in all sampling modes (Fig. 8). The closed loop controller in the towfish was found to be robust at these speeds. Initial tests in the Gulf of Maine were performed to examine depth follow mode at a sequence of increasing target depths (Fig. 8A). In this mode, the towfish was able to keep within 0.3 m of the desired depth.

We have found that the towfish can reach 105 m at 6 m/s (12 knots) when 50 m of fairing is used (Fig. 9). The towfish goes deeper at slower speeds (4 to 5 m/s) or with more fairing. A bare cable drag coefficient of 2.6 was inferred from the VPR depths measured at these speeds with 50 m of fairing and was used to predict cable shapes if 500 m of fairing were used (Fig. 9).

Total cable length was 800 m, with 100 m left on the winch and 15 m from the winch to the water surface, leaving 685 m in the water. The cable shapes at different towing speeds and fairing amounts were modeled using an 8.18-mm bare cable diameter. The model used cable tensions at the towfish that gave approximately 680 kg (1500 lb) at the winch. The lower three curves are for 500 m of fairing, and the tensions at the towfish were kept the same as in the 50-m fairing simulations. The extra tangential drag

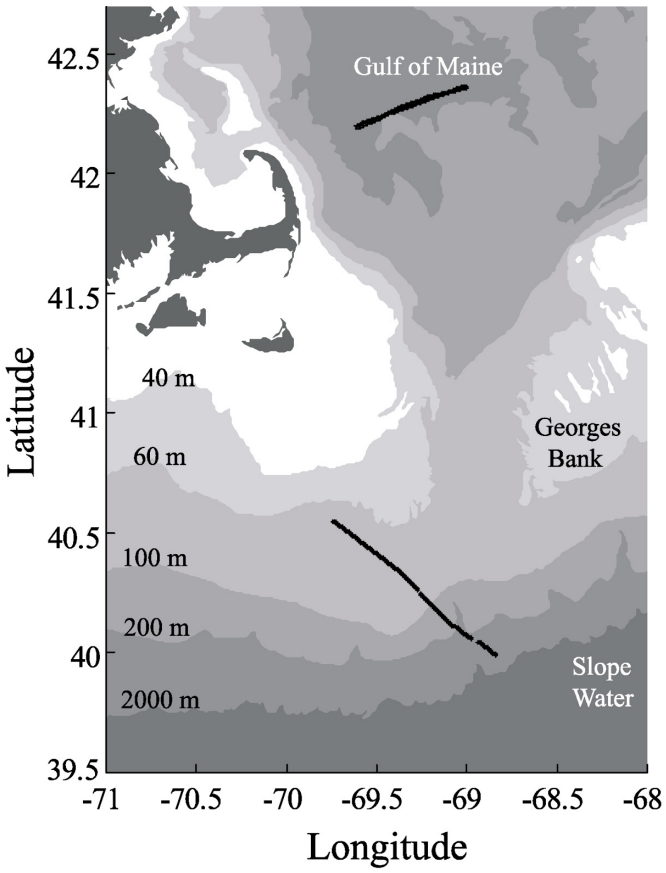

Fig. 7. Locations of VPRII field testing in the Gulf of Maine and shelf/slope water off Cape Cod, Massachusetts. Black lines denote ship track during VPRII deployments.

of the longer fairing increases the cable tension at the winch to 708, 904, and 1053 kg at 4, 5, and 6 m/s, respectively, which is within the safe working load of the cable (1134 kg).

For sampling out of the wake, we found that invoking a right rudder angle of 3° causes the towfish to move laterally to starboard 2 to 3 vessel-widths away from the wake. The towfish is thus able to sample in undisturbed water, where small-scale plankton patchiness is not destroyed by the ship's wake. During undulate mode, we have programmed the towfish to invoke 3° right rudder when reaching a depth of 30 m during its ascent. Thus in undulate mode, the towfish uses 0° rudder during its entire descent and while ascending up to 30 m. This pattern allows the towfish to avoid the wake.

Example data—Sensory data saved in the 1 Hz logging file can be plotted in real time as color dot plots, where dot color is proportional to variable values (e.g., temperature, Fig. 10).

The digital camera provides excellent images of a wide variety of plankton. Example images (ROIs) of the copepod *Calanus finmarchicus* show the oil storage sacs and other features such as body segmentation and setae (Fig. 11). We found the quality of images to be remarkable considering they were collected at a working distance of 50 cm and tow speed of 5 to

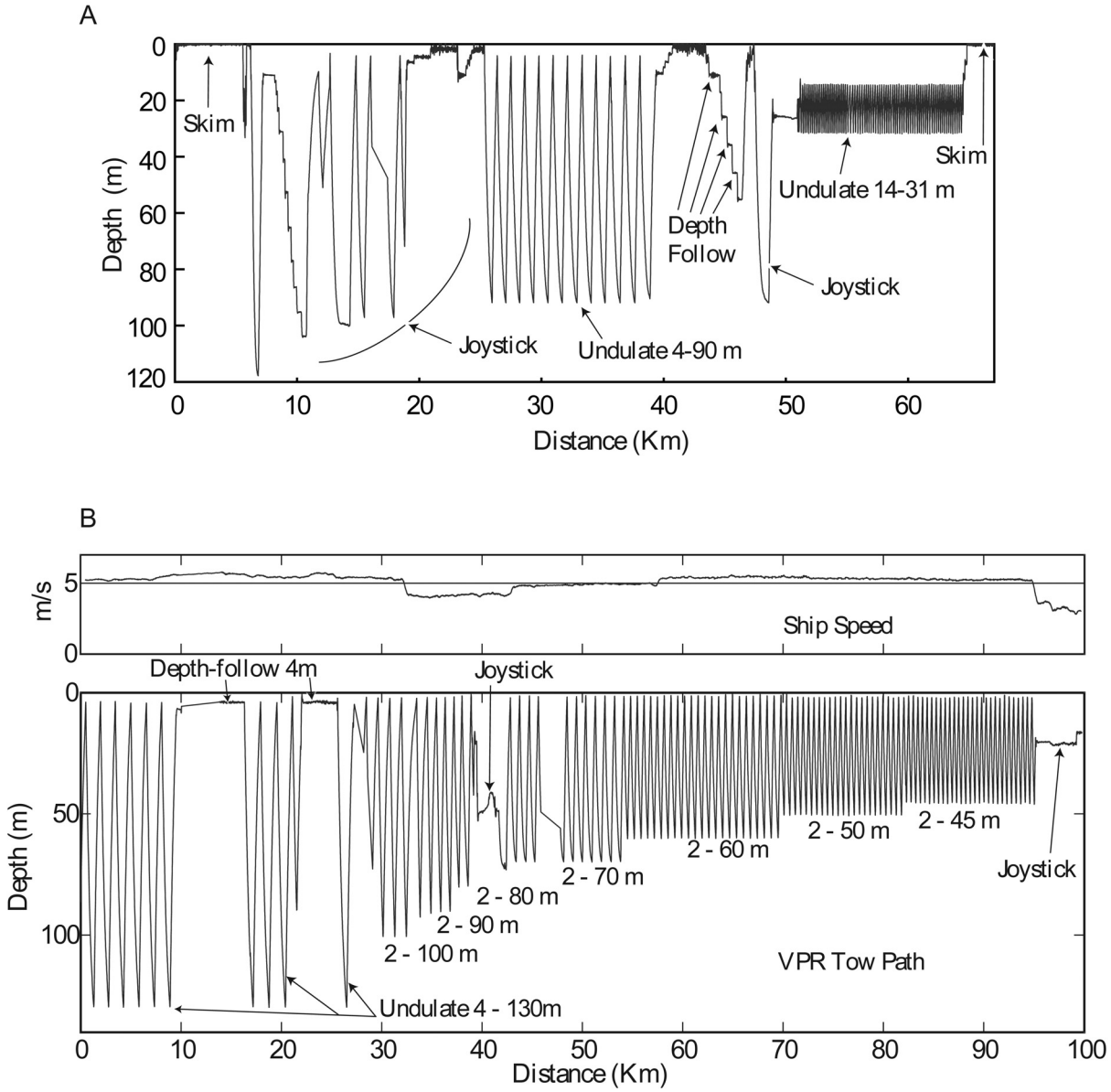

Fig. 8. (A) VPRII towfish depth profile during a test deployment in the Gulf of Maine. (B) Ship speed and VPRII towfish depth profile during a test deployment across the continental shelf edge south of Cape Cod. The towfish was in undulate mode most of the time except when in depth-follow mode at 4 m to avoid fishing gear and for two brief periods to test joystick mode. Ship speeds up to 6 m/s were achieved.

6 m/s. Given that the strobe pulse is 2 µs, a 5 m/s tow speed causes a spatial smearing of only 10 µm. High quality images of a wide variety of other organisms and marine snow have been obtained using the VPRII camera system (Fig. 12). The pteropod images were collected during an along-shelf transect from New York to Chesapeake Bay. Other images were collected by Japanese and German colleagues using similar VPR systems, which have the same model camera/strobe mounted on a V-fin depressor and towed at 4 m/s.

The distribution of the copepod *Calanus finmarchicus* (Fig. 11) found during a VPRII test tow in the Gulf of Maine revealed very high concentrations of this organism (max per second was 52,000/m^3; Fig. 13). This method of real-time taxa-specific data acquisition can be useful in determining plankton patch locations interactively.

Assessment of key features—Optical imaging systems can substantially improve our ability to sample plankton, including delicate forms, quickly and over a wide range of scales. The VPRII system meets our desired design criteria. The ability to tow at speeds up to 5 to 6 m/s allows rapid surveys of plankton and seston and the ability for deployment on transit legs of research vessels for opportunistic sampling. The use of a

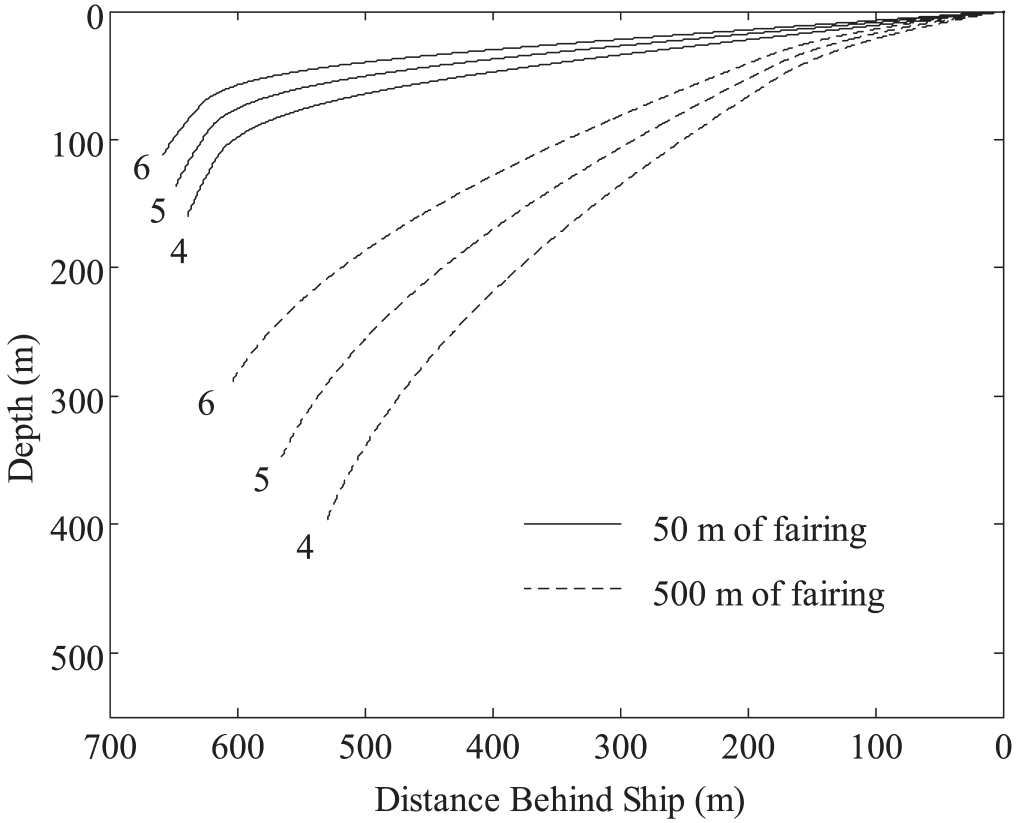

Fig. 9. Steady-state cable shapes for 685 m of cable in the water when towing the VPRII towfish. Curves are computed for 4, 5, and 6 m/s towing speeds and using 50 or 500 m of fairing. Curves were calibrated with data from the new VPRII field trials.

small winch and cable enables towing from smaller coastal vessels such as small research and fishing vessels (e.g., 12 m length). We have successfully deployed and retrieved the VPRII from WHOI's 12 m R/V *Asterias* and found stern deployment (versus side deployment) to be a simple operation because of the proximity to the water surface and alignment of the launch/recovery point with the centerline of the boat. Use on small vessels allows the sampler to be used for coastal and large lake/river surveys.

Automatic dynamic control of towfish lateral movement and undulation eliminates the need for towyoing via winch payout and haul-back. Lateral rudder movement and dynamically controlled aileron/elevator movement work well in allowing the VPRII to sample at a fixed depth or undulate between two specified depths, while avoiding the ship's wake and maintaining a horizontal attitude. The horizontal viewing angle permits better imaging of plankton, which are often oriented vertically. The abort mode enables the towfish to automatically avoid collision with the bottom.

The ability to move out of the ship's wake allows sampling of undisturbed small-scale plankton patches that would otherwise be destroyed. Research vessels moving at 10 knots create turbulent wakes that homogenize the upper 5 to 6 m (with penetration to 7 to 12 m), persist for kilometers behind the ship (Melsheimer et al. 1999; Trevorrow et al. 1994), and widen as $x^{1/5}$, where x is distance behind the ship (Reed and Milgram 2002). The latter formula indicates that the starboard edge of the turbulent wake will extend out 1.25 ship-widths at a position 1000 m aft of a 10-m wide ship (e.g., R/V *Oceanus*). Our observation that the VPR moves 2 to 3 vessel widths to starboard puts it well out of the way of the wake. Sampling in undisturbed water is important for studies of small-scale patchiness and behavioral postures.

The high resolution images, together with an imaged volume that is calibrated and undisturbed, allows for quantitative assessment of a wide variety of plankton taxa and seston. The large open space between the imaged volume and any towfish components, together with the tow bridle position on the opposite side of the towfish nose cone, reduces disturbance of the imaged volume and the possibility of avoidance by swimming zooplankton such as copepods.

Avoidance modeling —We have calculated the fluid strain rate at the location of the imaged volume for the VPRII. We modeled the flow disturbance in the imaged volume due to (1) lift, as the wing circulation, (2) the fuselage, as a Rankine half body, and (3) the wing thickness, as a line source. This modeling is a good approximation upstream of the fish, i.e., at the

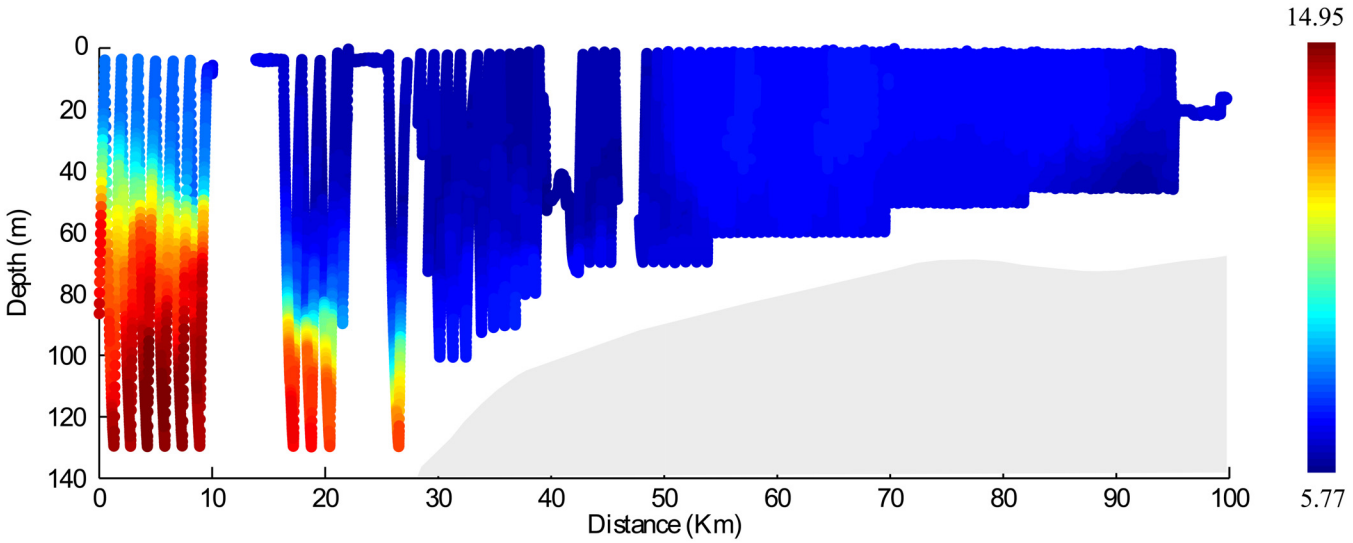

Fig. 10. Temperature distributions plotted in real time from the new VPRII during the transit across the shelf/slope edge south of Cape Cod (Fig. 7). Typical February well-mixed conditions were present on the shelf, with warmer (and saltier) slope water in the deeper water off the shelf edge.

location of the image volume. The assumed state was 680 kg (1500 lb) of lift on the wing and 5 m/s (10 knots) of flow. The shear is given as the principle strain rates from the computed strain rate tensor. The absolute values of the principle stain rates are 0.64/s, 0.08/s, and 0.06/s, respectively. These rates are less than the threshold shear rate needed to trigger escape reactions in copepods (0.8 to 56 s^{-1}) (Fields and Yen 1997; Haury et al. 1980), implying that the plankton are imaged prior to being disturbed. As further evidence, we also note that most organisms observed in the VPR images do not appear to be in a disturbed state (e.g., copepods in escape posture or distorted tentacle arrangements in ctenophores).

Discussion

The *Visual Plankton* interface program greatly facilitates data processing and display. Image processing, analysis, and plotting are done in 5 steps, using a graphical interface to guide the user through calibration, focus detection, classifier training, automatic identification, and data display.

An important objective of the VPRII design is to facilitate use of this optical technology. The VPR system has been made available free of charge to the general oceanographic research community as part of WHOI's ship equipment pool, allowing researchers to use this new method for high-resolution sampling of plankton and associated environment variables, thus helping to improve our understanding of pelagic systems.

The nature of optical imaging allows delicate plankton and seston to be sampled quantitatively (Ashjian et al. 2001; Davis et al. 1992*b*). Our present understanding of planktonic systems is largely from bottle and net samples, which collect robust organisms but destroy fragile forms such as gelatinous plankton and marine snow. This leads to a skewed view of pelagic ecosystem structure. For example, we have found that marine snow particles are often, by far, the most dominant form of particulate matter (including mesoplankton) in the ocean (Ashjian et al. 2001). The marine snow particles are home to a wide range of organisms and provide local substrate and microenvironments in the ocean where exchange of nutrients and biological activity may be rapid (Alldredge 1992; Alldredge and Jackson 1995; Alldredge and Silver 1988; Asper 1987; Eisma et al. 1990; Jackson et al. 1997; Lampitt et al. 1993; Stemmann et al. 2000). It is important therefore to quantify the abundance of these fragile forms. There are many other fragile plankton that are important to quantify as well including colonial protozoa (Caron and Swanberg 1990; Dennett et al. 2002), colonial phytoplankton (e.g., *Chaetoceros* socialis (Sieracki et al. 1998), *Rhizosolenia* mats (Villareal et al. 1999), and the colo-

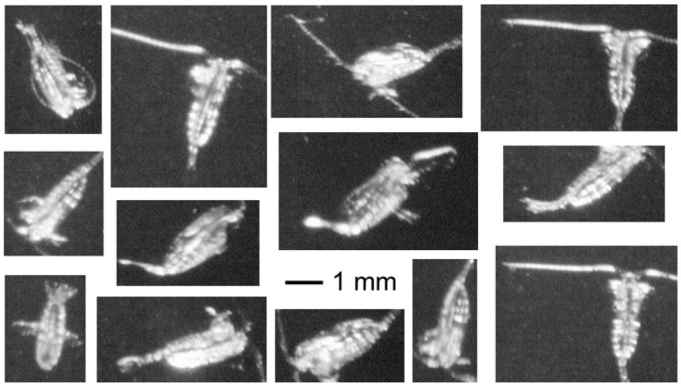

Fig. 11. Example images of copepods (*Calanus*) collected using the new digital VPR during a test deployment in the Gulf of Maine.

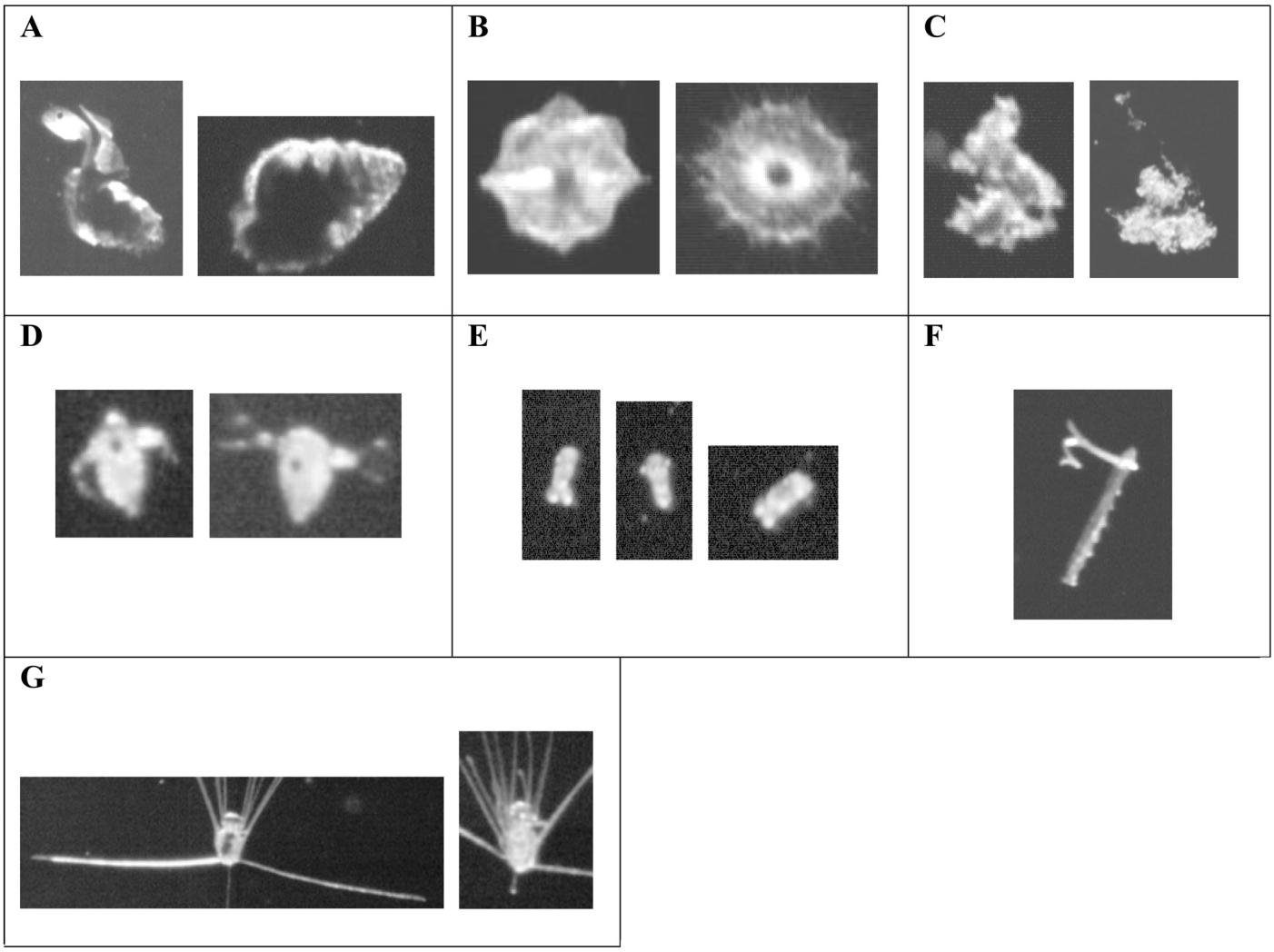

Fig. 12. Example images of various plankton captured by the digital VPRII camera while towing at 4 to 5 m/s. (A) Pteropods; (B) radiolarian; (C) marine snow; (D) cladocera; (E) rotifers; (F) polychaete; (G) Echinoderm larvae. (B-C) Japan Sea (from T. Ichikawa), (D-G) Baltic and North Seas (from A. Sell).

nial cyanobacteria, *Trichodesmium* (Capone et al. 1998; Carpenter and Roenneberg 1995; Davis et al. 1992*b*).

In addition to fragile forms, optical imaging also enables acquisition of high-resolution data on abundance of plankton, which can be compared with similar data on environmental variables including hydrography and fluorescence (e.g., Gallager et al. 1996). Such close comparison of plankton with small-scale environmental features can lead to a better understanding of the interaction of biology and physics at these scales and how plankton form observed patterns (Gallager et al. 2004).

The VPRII system has been designed and tested to provide rapid high-resolution data on abundance of plankton taxa and associated environmental variables. New insights into biological/physical mechanisms controlling plankton abundance have been made using the VPR (e.g., Ashjian et al. accepted-*a*, 2001, accepted-*b*; Benfield et al. 2000, 1996, 1998; Davis et al. 1996, 1992*b*, 2004; Gallager et al. 1996, 2004; Norrbin et al. 1996), and high abundance of fragile plankton (colonial algae and protozoa) have been found that significantly impact estimates of oceanic production and consumption (e.g., Dennett et al. 2002; Sieracki et al. 1998; Villareal et al. 1999). The increased capabilities of the VPRII and its availability to the research community will foster further exploration of plankton ecology in marine and freshwater habitats.

Comments and recommendations

Sampling at high speeds (6 m/s) to deep depths (>300 m) is obviously desirable and appears achievable, based on extrapolations from the testing we have done with the VPRII system at shallower depths (e.g., Fig. 9). The VPRII has been towed at 4 to 6 m/s to depths of 140 to 110 m, respectively, using 700 m of cable with 50 m of fairing. Although the system theoretically can sample to depths of 400+ m at 4 m/s using 500 m of

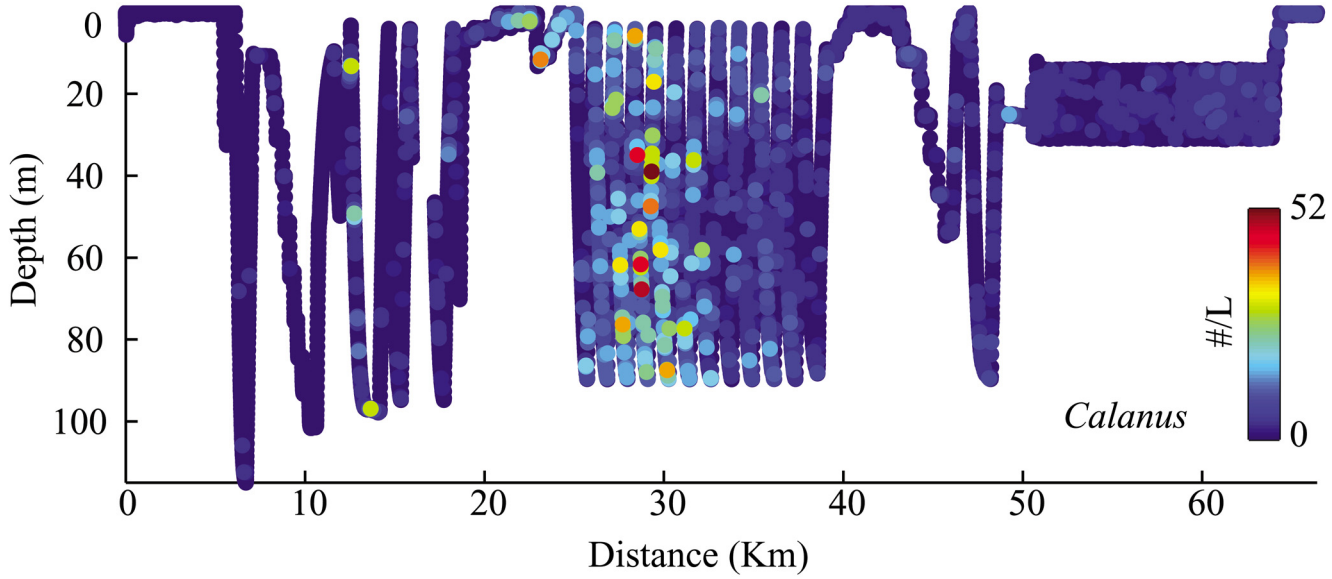

Fig. 13. Distribution of *Calanus finmarchicus* determined in real time while testing the VPRII system in the Gulf of Maine. Color dots are concentrations of copepods in 1-s time bins during the tow.

fairing and 1000 m of cable, such deployments have not yet been attempted. Further testing with more cable and fairing is required to confirm this capability. An additional 450 m of fairing would require use of a large winch, since only the top wrap of cable can contain fairing. The fairing also is time-consuming to install, which needs to be factored into the overall operating cost.

The VPRII has its own winch/cable and onboard equipment for control, acquisition, and image processing. The VPRII system (towfish, sheave, winch/cable, and two topside computers) fits into a single 20-foot container for shipping. Shipboard installation/setup typically takes a few hours by trained personnel.

Sampling volume—Although the volume imaged by the VPR is small compared with the volume filtered by a plankton net, the VPR can provide an equivalent or better estimate of plankton abundance, especially in shelf regions. Plankton nets typically oversample the number of organisms required for abundance estimation (Cassie 1968). The number of organisms captured is reduced to a manageable number for counting (e.g., 500 individuals) by taking a representative aliquot (e.g., from a Folsom splitter). VPR sampling can be viewed as a subsample taken along the tow path of a plankton net, giving an unbiased estimate of the sample mean (cf., Davis et al. 1996). In shelf areas, where abundances of total mesozooplankton (as determined by net sampling) are 10^3 to 10^4 m^{-3}, the VPR will count ~100 to 1,000 comparable (hardy) organisms over the distance traveled by an oblique net tow (e.g., 2 km). For plankton net surveys, such 2-km tows are used to estimate plankton abundance over the scale of the station spacing, e.g., 20 km. A VPR traveling at 5 m/s and undulating continuously along same survey line would count 1,000 to 10,000 comparable organisms per 20 km. Thus, in terms of number of organisms counted and length of tow (an important criterion for quantitative plankton sampling [Wiebe 1972]), the VPR will provide a more accurate estimate of plankton abundance at the scale of the station spacing. The VPR data also provides positions of each organism along the tow path, so that vertical and horizontal distributions are known. Using point-process methods, scales of patchiness can be determined down to the distance between adjacent video images (e.g., 20 cm at 6 m/s) (Davis et al. 1992*b*). In addition to shelf regions, we have used the VPR in oligotrophic waters, such as the Sargasso Sea and Japan Sea, to quantify plankton abundance at mesoscales and sub-mesoscales and patchiness scales down to 20 cm. On the downside, the taxonomic resolution provided by the present VPR is coarse, although distinctive and dominant species can be identified. At present, the VPR provides data on size structure together with coarse taxonomic composition.

Additional future improvements to the VPRII design include a color camera, which could help distinguish many plankton, a radial light source (such as a large ring illuminator), which would provide enhanced illumination to aid in identifications, and, eventually, three-dimensional imaging so that orientation of the plankton can be measured, eliminating ambiguity caused by two-dimensional projections in our current video imaging system and improving classification accuracy.

Limitations of the system include poor image quality in very turbid water, such as some bays and lakes. In these regions, the image quality may be corrected by changing the

working distance and lighting and incorporating recent image enhancement methods to adequately image plankton.

The current system also is limited to 250 m sampling depth and would require denser foam in the fins and fuselage to be used deeper. With denser foam, the practical depth limitation of this system is about 500 m at 8 knots. To achieve sampling depths > 500 m, wing surface area could be increased and slower towing speeds used. The absolute depth limitation for this technology is about 1000 m.

References

Alldredge, A. L. 1992. Marine snow in oceanic cycling. Encyclopedia of Earth System Science. Academic Press, San Diego, 3:139-147.

——— and G. A. Jackson. 1995. Aggregation in marine systems. Deep-Sea Res. II 42:1-8.

——— and M. W. Silver. 1988. Characteristics, dynamics and significance of marine snow. Prog. Oceanogr. 20:41-82.

Ashjian, C. J., S. M. Gallager, and S. Plourde. Accepted-*a*. Transport of plankton and particles between the Chukchi and Beaufort Seas during summer 2002, described using a Video Plankton Recorder. Deep-Sea Res. II.

———, C. S. Davis, S. M. Gallager, and P. Alatalo. 2001. Distribution of plankton, particles, and hydrographic features across Georges Bank described using the Video Plankton Recorder. Deep-Sea Res. II 48:245-282.

———, C. S. Davis, S. M. Gallager, and P. Alatalo. Characterization of the zooplankton community and size composition in relation to hydrography and circulation in the Sea of Japan. Deep Sea Res. II. (accepted-*b*).

Asper, V. L. 1987. Measuring the flux and sinking speed of marine snow aggregates. Deep-Sea Res. 34:1-17.

Benfield, M. C., C. S. Davis, and S. M. Gallager. 2000. Estimating the in-situ orientation of *Calanus finmarchicus* on Georges Bank using the Video Plankton Recorder. Plankton Biol. Ecol. 47:69-72.

———, C. S. Davis, P. H. Wiebe, S. M. Gallager, R. G. Lough, and N. J. Copley. 1996. Comparative distributions of calanoid copepods, pteropods, and larvaceans estimated from concurrent Video Plankton Recorder and MOCNESS tows in the stratified region of Georges Bank. Deep-Sea Res. II 43:1925-1946.

———, P. H. Wiebe, T. K. Stanton, C. S. Davis, S. M. Gallager, and C. H. Greene. 1998. Estimating the spatial distribution of zooplankton biomass by combining Video Plankton Recorder and single-frequency acoustic data. Deep-Sea Res. II 45:1175-1199.

Capone, D. G., and others. 1998. An extensive bloom of the N2-fixing cyanobacterium *Trichodesmium erythraeum* in the central Arabian Sea. Mar. Ecol. Prog. Ser. 172:281-292.

Caron, D. A., and N. R. Swanberg. 1990. The ecology of planktonic sarcodines. Rev. Aquat. Sci. 3:147-180.

Carpenter, E. J., and T. Roenneberg. 1995. The marine planktonic cyanobacterium Trichodesmium spp. photosynthetic rate measurements in the SW Atlantic Ocean. Mar. Ecol. Prog. Ser. 118:267-273.

Cassie, R. M. 1968. Sample design, p. 105-121. *In* D. J. Tranter [ed.], Zooplankton sampling. Monographs on oceanographic methodology. UNESCO.

Davis, C. S., S. M. Gallager, M. S. Berman, L. R. Haury, and J. R. Strickler. 1992*a*. The Video Plankton Recorder (VPR): Design and initial results. Arch. Hydrobiol. Beih. 36:67-81.

———, S. M. Gallager, M. Marra, and W. K. Stewart. 1996. Rapid visualization of plankton abundance and taxonomic composition using the Video Plankton Recorder. Deep-Sea Res. II 43:1947-1970.

———, S. M. Gallager, and A. R. Solow. 1992*b*. Microaggregations of oceanic plankton observed by towed video microscopy. Science 257:230-232.

Davis, C. S., Q. Hu, S. M. Gallager, X. Tang, and C. J. Ashjian. 2004. Real-time observation of taxa-specific plankton distributions: An optical sampling method. Mar. Ecol. Prog. Ser. 284:77-96.

Dennett, M. R., D. A. Caron, A. E. Michaels, M. Church, S. M. Gallager, and C. S. Davis. 2002. Video Plankton Recorder reveals high abundance of colonial radiolaria in surface waters of the central north Pacific. J. Plankton Res. 24:797-805.

Eisma, D., and others. 1990. A camera and image-analysis system for in situ observation of flocs in natural waters. Netherl. J. Sea Res. 27:43–56.

Fields, D. M., and J. Yen. 1997. The escape behavior of marine copepods in response to a quantifiable fluid mechanical disturbance. J. Plankton Res. 19:1289-1304.

Froese, R., K.-G. Barthel, W. Welsch, M. Rolke, C. Schubert, B. Herrnann, S. Mees, D, Schnack, and J. Lenz. 1990. Development of an underwater video system for recording of ichthyoplankton and zooplankton. ICES CM 1990/L: 90. 6 pp.

Gallager, S. M., C. S. Davis, A. W. Epstein, A. Solow, and R. C. Beardsley. 1996. High-resolution observations of plankton spatial distributions correlated with hydrography in the Great South Channel, Georges Bank. Deep-Sea Res. II 43: 1627-1664.

———, H. Yamazaki, and C. S. Davis. 2004. Contribution of fine-scale vertical structure and swimming behavior to formation of plankton layers on Georges Bank. Mar. Ecol. Prog. Ser. 267:27-43.

Haury, L. R., D. E. Kenyon, and J. R. Brooks. 1980. Experimental evaluation of the avoidance reaction of *Calanus finmarchicus*. J. Plankton Res. 2:187-202.

———, J. A. McGowan, and P. H. Wiebe. 1978. Patterns and processes in the time-space scales of plankton distributions, in spatial patterns in plankton communities, p. 277-327. *In* J. H. Steele [ed.], Spatial patterns in plankton communities. Plenum Press.

Herman, A. W. 1992. Design and calibration of a new optical plankton counter capable of sizing small zooplankton. Deep-Sea Res. 39:395-415.

Holliday, D. V., R. E. Pieper, and G. S. Kleppel. 1989. Determination of zooplankton size and distribution with multifrequency acoustic technology. J. Cons. Int. Explor. Mer. 41:226-238.

Hu, Q., and C. S. Davis. Automatic plankton image recognition with co-occurrence matrices and support vector machine. Mar. Ecol. Prog. Ser., (in press).

Jackson, G., R. E. Maffione, D. K. Costello, A. L. Alldredge, B. E. Logan, and H. G. Dam. 1997. Particle size spectra between 1 μm and 1 cm at Monterey Bay determined using multiple instruments. Deep-Sea Res. 44:1739-1767.

Lampitt, R. S., K. F. Wishner, C. M. Turley, and M. V. Angel. 1993. Marine snow studies in the Northeast Atlantic Ocean: distribution, composition and role as a food source for migrating plankton. Mar. Biol. 116:689-702.

Lenz, J., and others. 1995. The ichthyoplankton recorder: a video recording system for in situ studies of small-scale plankton distribution patterns. ICES J. Mar. Sci. 52:409-417.

Melsheimer, C., H. Lim, and C. Shen. 1999. Observation and analysis of ship wakes in ERS SAR and SPOT images. Proc. 20th Asian Conf. Remote Sensing: 1:554-559.

Norrbin, M. F., C. S. Davis, and S. M. Gallager. 1996. Differences in fine-scale structure and composition of zooplankton between mixed and stratified regions of Georges Bank. Deep-Sea Res. II 43:1905-1924.

Ohman, M. D., and P. E. Smith. 1995. A comparison of zooplankton sampling methods in the CalCOFI time series. Reports of California Cooperative Oceanic Fisheries Investigations [CALC CALCOFI REP.] 36:153-158.

Reed, A. M., and J. H. Milgram. 2002. Ship wakes and their radar images. Ann. Rev. Fluid. Mech. 34:469-502.

Samson, S., T. Hopkins, A. Remsen, L. Langebrake, T. Sutten, and J. Patten. 2001. A system for high-resolution zooplankton imaging. IEEE J. Ocean. Eng. 26:671-676.

Sherman, K. 1980. MARMAP, a fisheries ecosystem study of the Northwest Atlantic fluctuations in ichthyoplankton-zooplankton components and their potential for impact on the system, p. 3-37. *In* Diemer, F.P., F.J. Verberg and D.Z. Mirkes, [eds.], Advanced concepts in ocean measurements of marine biology. Univ. South Carolina Press.

Sieracki, M., D. Gifford, S. M. Gallager, and C. S. Davis. 1998. Observations on a dense patch of the diatom, *Chaetoceros socialis*, on the southern flank of Georges Bank: Distribution, colony structure and grazing losses. Oceanography 11:30-35.

Stemmann, L., M. Picheral, and G. Gorsky. 2000. Diel variation in the vertical distribution of particulate matter (0.15 mm) in the NW Mediterranean Sea investigated with the underwater video profiler. Deep-Sea Res. 47:505-531.

Tang, X., and others. 1998. Automatic plankton image recognition. Artif. Intell. Rev. 12:177-199.

Thwaites, F. T., and C. S. Davis. 2002. Development of a towed flyable fish for the Video Plankton Recorder. Oceans '02 Conference Proceedings 3:1730-1736.

Trevorrow, M. V., S. Vagle, and D. M. Farmer. 1994. Acoustical measurements of microbubbles within ship wakes. J. Acoust. Soc. Am. 95:1922-1930.

Villareal, T. A., C. Pilskaln, M. Brzezinski, F. Lipschultz, M. Dennett, and G. B. Gardner. 1999. Upward transport of oceanic nitrate by migrating diatom mats. Nature 397: 423-425.

Wiebe, P. H. 1972. A field investigation of the relationship between length of tow, size of net, and sampling error. J. Cons. Perm. Int. Expl. Mer. 34:268-275.

——— and others. 2002. BIOMAPER-II: An integrated instrument platform for coupled biological and physical measurements in coastal and oceanic regimes. IEEE J. Ocean. Eng. 27:700-716.

Submitted 5 October 2004
Revised 10 November 2004
Accepted 30 November 2004